# Hierarchical Grasp Controller using Tactile Feedback

Massimo Regoli, Ugo Pattacini, Giorgio Metta and Lorenzo Natale

***Abstract*— Grasp stability is a challenging problem in robotics. It needs to be robust to external perturbations and adapt to unknown objects. While performing a stable grasp, grip strength control can be a desirable property for many applications. We present an approach for stable object grasping and simultaneous grip strength control using tactile feedback, which is able to deal with unknown objects of different shape, size and material. We develop a generic method that exploits the structure of an anthropomorphic hand to be simple and effective. Our approach uses techniques from classical control theory to develop a controller in charge of coordinating the fingers for achieving grasp stabilization and grip strength control. Then, we applied a machine learning method based on Gaussian mixture model regression, with the aim of further improving stability and increasing robustness to external perturbations. The method has been validated on the iCub robot. Experimental results show the effectiveness of our approach.**

## I. Introduction

Grasp stability is a fundamental topic in robotics. A stable grasp is needed in order to prevent objects from slipping and is the basis for manipulation. In order to achieve this objective, many works adopt analytical solutions (see [1] for a review). Indeed, when the hand kinematics and the contacts between the hand and the object are known, it is possible to determine if the grasp is in force or form closure [2], which is sufficient for stability. However, many difficulties arise when the object model is unavailable or partially known. As a result, grasps cannot be pre-planned, and the typical strategy is to make extensive use of sensors in order to deal in real-time with environmental uncertainties.

In this context, tactile feedback can reveal object properties which could be hardly detected by other sensors (e.g., object softness and shape at the points of contact) and perform proper reactive strategies. Different works pointed out the importance of exploiting such a rich set of sensory information while manipulating objects [3] [4]. As a result, in order to deal with grasp stability many tactile-based methods have been developed.

This research has received funding from the European Union's Seventh Framework Programme for research, technological development and demonstration under grant agreement No. 610967 (TACMAN).

The authors are with the iCub Facility, Istituto Italiano di Tecnologia, via Morego, 30, 16163 Genova, Italy email: {massimo.regoli, ugo.pattacini, giorgio.metta, lorenzo.natale}@iit.it

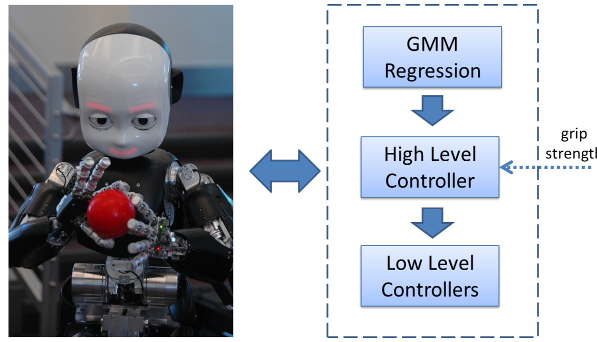


Fig. 1: Schema of our hierarchical approach. Arrows represent information flow.

One way to approach the problem is by focusing on the selection of feasible points of contact to avoid unstable grasps. Typically, these methods rely, at least partially, on vision [5] or make assumptions about the object model [6]. Other works still aim at evaluating the grasp stability [7], but do not provide active strategies to improve the grasp. Another approach – considered in this work – is to adjust an initial unstable grasp to a stable one. In this respect, Sauser *et al.* [8] use a model representing stable grasps in order to infer the hand configuration and pressure at the fingertips given the estimated normals of contact between the hand and the object. Li *et al.* [9] use a similar model to regulate the stiffness at the fingertips depending on the tactile readings and on the relative positions of the points of contact. In both works, stable grasps are learned with the help of a human demonstrator. Indeed, learning by demonstration proves to be helpful in order to reduce the complexity of tasks where many variables are involved [10] [11]. Dang *et al.* [12] build a database of stable grasps using a simulator. When an object is grasped they search for the nearest stable grasp in the database.

Usually grasp stability approaches implicitly define the grip strength to be applied to the object. This is sufficient if the only objective is to achieve a stable grasp, however, it strongly limits any further grip strength control on the object. An independent control of the grip strength is beneficial for several tasks, like slip control or object exploration (e.g., to explore object properties like softness and type of material). However, the problem of controlling the grip strength while maintaining a stable grasp is hard. Indeed, due to several nonlinearities in the system, a simple proportional variation of the forces applied to the object does not guarantee that stability is maintained. Jalani *et al.* [13] use a model reference approach where a virtual mass-spring damper system is used to design a robust active compliant control. However, the model parameters need to be tuned for every different object class.

In this work we combine techniques from control theory and machine learning in a hierarchical control. The novelty of our method is that it decouples the problem of grip strength control and grasp stability, providing an effective framework where both objectives are achieved at the same time. Our solution can be applied to unknown objects of different size, shape and material, without the need for object specific tuning. We deal with precision grasps [14], where only the fingertips are in contact with the object.

We validated our method on the humanoid robot iCub [15], performing experiments to demonstrate reliable control of grip strength and improvement of grasp stability.

In the next section we present the methodology used to solve the problem. In section III we describe the platform, the experiments carried out to validate our method and the related results. Finally, in section IV we draw the conclusions of this work.

## II. Methodology

We propose a hierarchical method made of three main components (Fig. 1):

- A low-level controller framework, composed of a force controller for each finger.
- A high-level controller, which determines the force reference values for each finger in order to stabilize the grasp while maintaining a given grip strength. At this stage, the controller is simplified by taking advantage of the anthropomorphic structure of the hand.
- A Gaussian mixture regression model, which exploits the high-level controller to further improve stability by changing the hand configuration. We made use of learning by demonstration in order to describe the space of stable grasps.

The data required for the Gaussian mixture model (GMM) training process are significantly reduced in quantity with respect to other methods considering that the relationship between the forces at the fingertips do not need to be learned, since the underlying high level controller takes care of that.

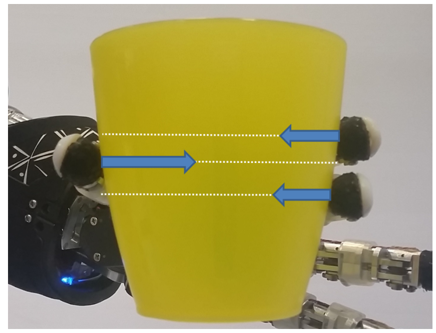

Fig. 2: When the grasp is stable the force directions are assumed to be parallel.

In this work we only focus on three-finger precision grasps. We make extensive use of tactile feedback, and we define the vector $\mathbf{f} \equiv [f_{th} \;\; f_{ind} \;\; f_{mid}] \in \mathbb{R}^3$ containing the tactile reading at each fingertip. Since we deal with precision grasps, the palm is not taken into consideration.

In the following subsections we first give our definition of grip strength for anthropomorphic hands, then we detail our strategy.

### A. Grip strength

Inspired by work on humans [16], we define the grip strength as the measure of force exerted on the object by the thumb (on one side) and the index and middle fingers (on the other side). Ideally, the tactile readings $f_i$ at each fingertip are proportional to the magnitude, $F_i$, of the real forces. However, tactile sensors are subject to calibration errors, noise, hysteresis, and they may detect only normal forces. Therefore, we model $f_i$ as:

$$f_i = k \cdot F_i + e, \tag{1}$$

where $k$ is a proportional value converting the tactile sensors output (in our case capacitance) into forces (newtons), while $e$ represents a random variable having a normal distribution and equal variance on each fingertip, i.e., $e \backsim \mathcal{N}(0, \sigma)$, $f_i \backsim \mathcal{N}(k \cdot F_i, \sigma)$. In addition, we set $f_{IM} = f_{ind} + f_{mid} \backsim \mathcal{N}(k \cdot F_{IM}, 2\sigma)$.

We further assume that when the grasp is stable, the directions of all applied forces are parallel (Fig. 2). Under this assumption we define the tactile measure of the actual grip strength as $g = k \cdot F_{th} = k \cdot F_{IM}$, and its estimate $\hat{g}(\mathbf{f})$ as the most probable value of $g$ given the observations $f_{th}$ and $f_{IM}$:

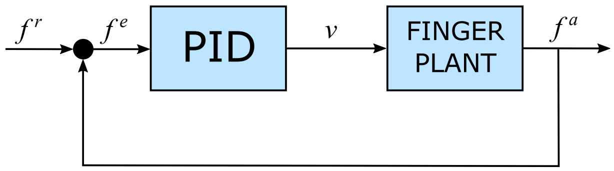


Fig. 3: Force control schema: $f^r$ represents the tactile reference, while $f^a$ is the tactile readings at the fingertip.

$$\hat{g}(\mathbf{f}) = \underset{g}{\operatorname{argmax}}\, p(g|f_{th}, f_{IM}), \tag{2}$$

where for sake of simplicity we omit random variables in the notation. Using Bayes' rule, and assuming $p(g)$ to be uniformly distributed, we can equivalently maximize the likelihood function:

$$\hat{g}(\mathbf{f}) = \underset{g}{\operatorname{argmax}}\, p(f_{th}, f_{IM}|g). \tag{3}$$

According to our error model, we can rewrite $\hat{g}(\mathbf{f})$ as follows:

$$\begin{aligned}
\hat{g}(\mathbf{f}) &= \underset{g}{\operatorname{argmax}}(p(f_{th}, f_{IM}|g)) \\
&= \underset{g}{\operatorname{argmax}}\left(p(f_{th}|g) \cdot p(f_{IM}|g)\right) \\
&= \underset{g}{\operatorname{argmax}}\left(k(\sigma) \cdot e^{-(f_{th}-g)^2/2\sigma^2} \cdot e^{-(f_{IM}-g)^2/4\sigma^2}\right) \\
&= \underset{g}{\operatorname{argmin}}\left(\frac{(f_{th}-g)^2}{2\sigma^2} + \frac{(f_{IM}-g)^2}{4\sigma^2}\right) \\
&= \frac{2}{3} \cdot f_{th} + \frac{1}{3} \cdot (f_{ind} + f_{mid}),
\end{aligned} \tag{4}$$

where $k(\sigma)$ is a quantity unrelated to $g$. This result points out how the estimate $f_{th}$ is more reliable than $f_{IM}$. This is because $f_{IM}$ sums up noise affecting both the index and the middle fingertips.

### B. System components: force controllers

As first step we developed a framework made of a PID force controller for each finger (Fig. 3). The input to the plant is the voltage $v$ to the motor actuating the proximal joints, while the feedback is the tactile readings at the fingertip. The other joints (i.e. those actuating the distal and abduction movements) are controlled independently in position. Using this approach we identified the system parameters under different conditions (material property, initial force value) and apply techniques from control theory to identify the gains of a controller that is stable in all working conditions.

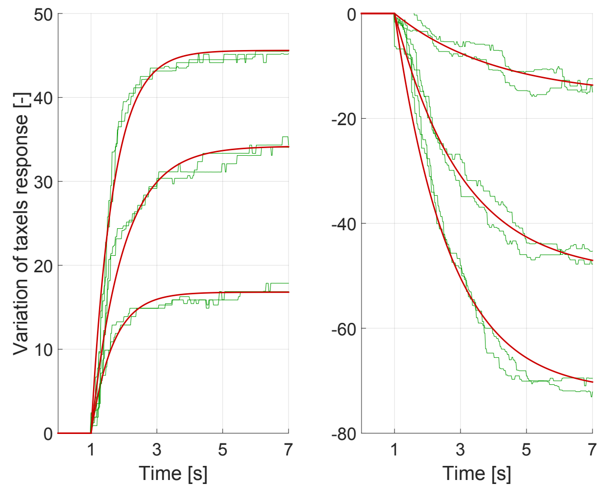


Fig. 4: Plant validation. The actual responses of the system (in green) and the simulated response (in red) to three step-up (left) and step-down (right) input signals.

We identified the system by placing the index fingertip in constant contact with an object and by applying step-wise input voltage while measuring the profile of tactile feedback. We executed several experimental sessions varying the initial tactile values, the height of the voltage step and the object used. The main goal was to better characterize the plant for different materials (in particular different degrees of softness) and in diverse working zones, where the presence of non-linearities affect differently the overall performance. The results of these experiments demonstrate that the response of the system is repeatable, given the same initial conditions.

We approximate the response of the system in the different conditions with a set of 32 first order $G_i(s)$ systems spanned by pairs of stable poles $\tau_{p,i}$ and DC gains $K_i$. In formula:

$$G_i(s) = \frac{K_i}{\tau_{p,i} \cdot s + 1} \tag{5}$$

Each transfer function, characterized by the parameters $(K_i, \tau_{p,i})$, was successfully validated using further repetitions of the related experiment, as shown in Fig. 4.

We then used the Robust Control Toolbox of MATLAB, to compute, using all the pairs $(K, \tau_p)$ as input, the optimal PID gains for the controller. These allowed us to obtain gains that perform better (in terms of system stability and step response) in all the working conditions.

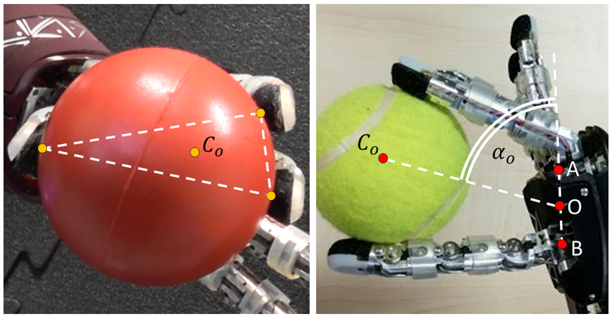

Fig. 5: The object center, $C_o$, is defined as the centroid of the triangle identified by the three points of contact (left). The object position, $\alpha_o$, is defined as the angle between the vectors $\vec{OC_o}$ and $\vec{OA}$ (right). $A$ and $B$ are set at the base of the middle finger and the thumb, respectively, while $O$ lies at midpoint between $A$ and $B$.

### *C. System components: high-level controller*

This layer coordinates the fingers by sending proper tactile references to the low-level controllers, with the aim of stabilizing the grasp while maintaining a given grip strength. The controller enforces the constraint in (4) and modulates the forces to control the position of the object with respect to a frame attached to the hand. We define the object center, $C_o$, as the centroid of the triangle identified by the three points of contact between the fingertips and the object (Fig. 5). Instead of controlling $C_o$ in the three-dimensional space, we simplify the problem by considering that:

- at this stage, only proximal joints are free to move;
- in an anthropomorphic hand the rotational axis of the proximal joints are nearly parallel to each other.

As a result, $C_o$ ends up moving along a curve path when the object is controlled by our system, which is, in turn, responsible for regulating the final position of the fingers in contact. In order to locate $C_o$ along this path, we define the object position, $\alpha_o$, as the angle shown in Fig. 5. For our purposes, we are not interested in controlling any possible rotation of the object around $C_o$. For this reason we always set the tactile references of the index and the middle fingers equal.

The controller objective is to compensate the error between the reference object position, $\alpha_o^r$, and the actual object position, $\alpha_o^a$. In order to overcome such an error we use a further PID controller dealing with the following quantity:

$$u(\mathbf{f}) = f_{ind} + f_{mid} - f_{th}. \tag{6}$$

The quantity $u(\mathbf{f})$ represents our estimate of the resultant force applied to the object by the fingers. Ideally, for $u > 0$, the object will move towards the thumb (i.e. $\dot{\alpha_o} > 0$), whereas for $u < 0$ the object will move towards the index and the middle fingers (i.e. $\dot{\alpha_o} < 0$); in practice, the equilibrium will be satisfied for $u = u_{eq} \neq 0$. As depicted in Fig. 6, the high level PID controller takes the object position error $\alpha_o^e = \alpha_o^r - \alpha_o^a$ as input signal and yields suitable values of the control signal $u$ to be partitioned among the three fingers force controllers with the goal of driving $\alpha_o^e$ to zero. Such a control partition is found as follows: once a specific equilibrium index $u^*$ is requested, and given a desired grip strength $g^*$, the set of tactile references to be sent to the underlying low level controllers can be calculated by solving the following system of equations:

$$\begin{cases} u(\mathbf{f}) = u^* \\ g(\mathbf{f}) = g^* \\ f_{ind} = f_{mid} \end{cases}. \tag{7}$$

This leads to:

$$f_{ind} = f_{mid} = \frac{g^*}{2} + \frac{u^*}{3}, \; f_{th} = g^* - \frac{u^*}{3}. \tag{8}$$

The resulting control schema is shown in Fig. 6.

### *D. System components: stable pose learning*

At the top layer in the hierarchy a GMM provides the values of $\alpha_o^*$ and the remaining joints of the hand, $\mathbf{\Theta_{np}^*}$, that lead to the best grasp in terms of stability. The GMM learns a probabilistic model of a set of stable grasp poses. This model is trained by demonstration, i.e., a human operator marks stable grasps, avoiding grasp configurations that are likely to cause object instability, such as a nonzero momentum applied by the fingers or unstable contacts between the object and the fingertips. In addition, to facilitate consequent manipulation tasks, we considered preferable grasp configurations that are far from joint limits and in which the contact points were as close as possible to the center of the fingertips.

The features that we chose as variables of the GMM are the set $\mathbf{\Theta_{np}}$, the object position $\alpha_o$ and the set $\mathbf{L}$ of lengths of the edges of the triangle defined by the points of contact (Fig. 5). We indicate this set of features used to train the model as $\mathbf{G} \equiv < \mathbf{\Theta_{np}}, \alpha_o, \mathbf{L} >$. The likelihood of a given grasp configuration $\mathbf{G}^*$ under a GMM $\Omega$ with $m$ components is calculated as follows:

$$p(\mathbf{G}^*|\Omega) = \sum_{i=1}^{m} \pi_i \mathcal{N}(\mathbf{G}^*|\mu_\mathbf{i}, \mathbf{\Sigma_i}) \tag{9}$$

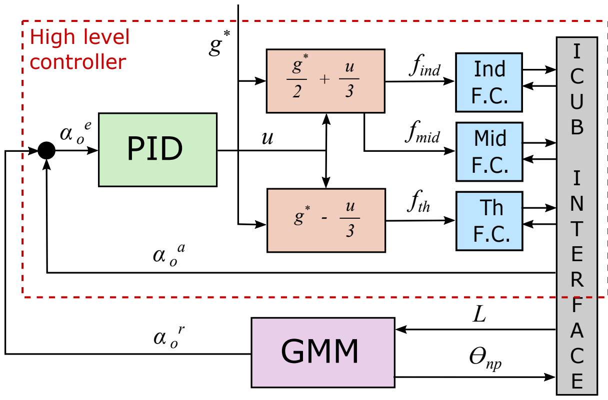


Fig. 6: Final control schema including all the components of our method. The cyan boxes represent the force controllers, while the red dashed line identifies the high level controller.

where $\pi_i$ is the prior of the $i^{th}$ Gaussian component and $\mu_{\mathbf{i}}$ and $\mathbf{\Sigma_i}$ are its related mean and variance; $p(\mathbf{G}^*|\Omega)$ can be considered as a measure of likelihood of stability.

We further characterize $\mathbf{G}$ as $\mathbf{G} = \mathbf{Q} \cup \mathbf{R}$, that is, the union of two subsets. The first, denoted by $\mathbf{Q} = \{\mathbf{L}\}$, contains features that encode the structure of the object and barely change while manipulation takes place. As a result, they cannot be controlled. The second, denoted by $\mathbf{R} = \{\mathbf{\Theta_{np}}, \alpha_o\}$, contains all features that can be controlled.

The main idea is that, given a grasp on an object and its corresponding set of features, $\mathbf{Q}^*$, the model can be exploited in order to infer a set of features $\mathbf{R}^*$ that maximizes $p(\mathbf{G}|\Omega)$, and, consequently, makes the grasp as stable as possible. The features $\mathbf{R}^*$ can be easily retrieved by taking the expectation over the conditional distribution $p(\mathbf{R}|\mathbf{Q}^*, \Omega)$, which can be expressed in closed form [8] [9]. Once $\mathbf{R}^*$ is given, we know where to steer the proximal joints of the hand using the high level controller, whereas the remaining joints are controlled in position to reach their set-point $\mathbf{\Theta^*_{np}}$. In Fig. 6 is reported the final control schema which includes the GMM regression.

## III. Experiments

To validate our work we used the humanoid robot iCub. The hands of the iCub are endowed with 9 joints. Each of the 5 fingers has 12 capacitive tactile sensors on the tip [17]. We estimate the force at each fingertip by taking the magnitude of the vector obtained by summing up all the normals at the sensor locations weighted by the sensors response.

For training the GMM we used a set of 10 objects of different size, shape and material (Fig. 7). For each object we carried out 6 different grasps, each starting from a different hand pose. The object position, $\alpha_o$, and all the joint values in $\mathbf{\Theta_{np}}$ were chosen manually in order to find a pose that was visually determined to be stable under the action of the high level controller. After each grasp we stored the model features $\mathbf{G}$. The 60 feature vectors were used to train the GMM.

Fig. 7: The objects used to train the GMM.

During the training process we explored as much as possible the space $\mathbf{L}$ of the distances between the points of contact. In this way, the GMM regression becomes reliable and robust with respect to the query point $\mathbf{Q}$. In our experiments, the number of Gaussian components, $m$, is set to 2 using the *Bayesian information criterion*. Before the training process, data was normalized to zero mean with range [-1, 1].

We run several experiments in order to show the effectiveness of our method. We evaluated the tracking performance of the high-level controller in terms of object position and grip strength control and the performance of the grasping adaptation in terms of grasp stability and pose quality.

In each experiment we used the four objects shown in Fig. 8. These objects were chosen because they have different size, shape and are made of different material. In addition they are different from the ones used for the PID force controller tuning and from the ones used for the GMM training. During the experiments the encoders and the tactile data were sampled at 50 Hz.

### A. Object position tracking

For each object we used the high level controller to control the object position by tracking sine wave reference signals. Since the GMM regression is not used in this experiment, only proximal joints are controlled while the other joints are maintained fixed at a constant position. During the experiments both the target and the actual object position were collected.

Fig. 8: The objects used for the experiments.

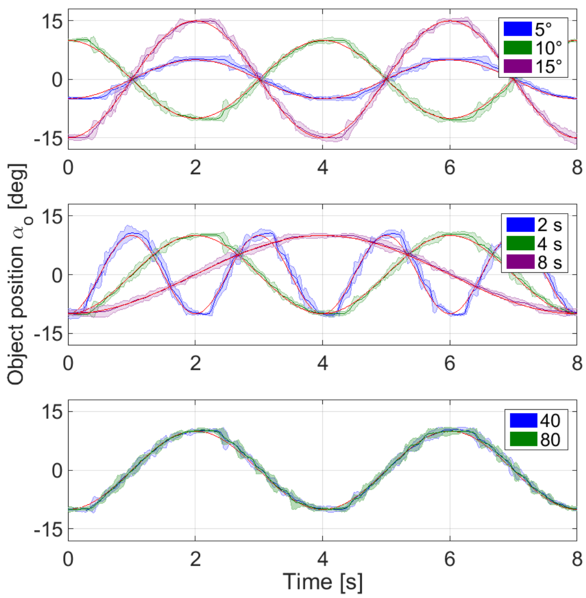


Fig. 9: Object position tracking performance. For each setting, the target object position (in red) and the mean and the confidence interval at 95% over the different objects of the actual object position are shown. We run different trials where we varied the sine wave amplitude (top), period (middle) and the grip strength (bottom) starting from a reference sine wave with amplitude $10°$, period 4 sec. and grip strength 80.

Fig. 9 shows the results for all the wave signals considered. In each experiment the controller was able to track the reference reliably and with low error.

## *B. Grip strength control*

We evaluate the performance of the controller to maintain a desired grip strength on the object. We compare our approach against a baseline, simpler strategy in which the fingers move towards the object at constant speed and stop as soon as contact is detected on the fingertips. The grip strength on the object is measured

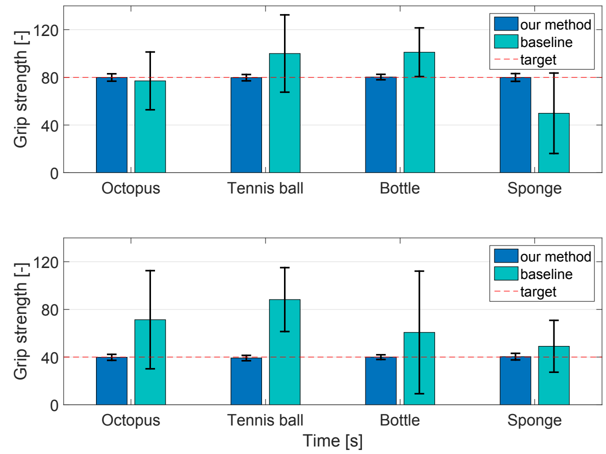


Fig. 10: Grip strength control. The mean and the confidence interval at 95% over the different trials are shown. Notice that our approach allows controlling the grip strength with higher realiability and accuracy than the baseline.

using the tactile sensors and compared against the grip strength obtained with our controller.

To evaluate our approach for each object, we tried to reach two grip strength references, namely 40 and 80. For the baseline, in order to achieve a given grip strength $x$, we simply set the force thresholds to the fingers, that is $x$ to the thumb, and $\frac{x}{2}$ to both the index and the middle fingers. For each combination of object and grip strength reference we run 5 trials of the experiment, starting from a different hand pose.

In Fig. 10 are shown the results of the experiment. Notice that the grip strength achieved by the baseline is generally higher than the target and quite unpredictable (i.e. it is affected by high variance). Overshooting is probably due to a delay in the tactile response, showing that a proper force control is needed. By contrast, our method is able to maintain the desired grip strength with accuracy, independently from the object and from the target reference.

## *C. Grasp stability*

To measure the grasp stability we perturbed the hand after the grasp adaptation obtained using the GMM regression model. In particular, we carried out 5 experiments per object and then compared the results with the same baseline controller used for the previous experiment. The perturbation consisted in shaking the hand by means of a sine wave signal sent as position reference to one of the wrist joints. The sine wave had a period of 0.5 seconds, an amplitude of 5 degrees

| Success rate | Octopus | Tennis ball | Bottle | Sponge |
|---|---|---|---|---|
| Our method | 5/5 | 4/5 | 5/5 | 5/5 |
| Baseline | 4/5 | 1/5 | 2/5 | 4/5 |

TABLE I: Results of the stability performance experiment. For each object the table shows the number of times that the object did not fall after the perturbation.

and a total duration of 1 second. In order to make the comparison fair, the same series of hand starting poses was used for both methods under analysis. As measure of stability we counted the number of times in which the object did not fall as a result of the perturbation.

Table I shows that grasps obtained with our method were robust to perturbations, even when dealing with slippery objects, like the tennis ball and the bottle. In contrast, the baseline method was unreliable with these objects, meaning that the re-grasp strategy was effective. On the other hand, the performance of both methods on soft objects is similar, since these objects hardly slip independently of the hand configuration.

### D. Hand pose quality

With this experiment we demonstrate that the re-grasp strategy provided by the GMM leads to hand configurations that are preferable for manipulation purposes. Indeed, when an object is randomly grasped, the finger might end up in a configuration that is close to the joint bounds, or in which contact between the object and the fingertips is close to the borders of the fingertip. In such cases, any consequent manipulation would be limited. In order to quantitatively describe this limiting condition, we introduced the following indexes:

- The *bounds* penalty index:
$$\eta_B = \sum_{i \in \boldsymbol{\Theta}} \frac{1}{\Theta_i - \Theta_{mini}} + \frac{1}{\Theta_{maxi} - \Theta_i}, \qquad (10)$$
where $\boldsymbol{\Theta}$ is the set of hand's joints, while $\Theta_{mini}$ and $\Theta_{maxi}$ represent lower and upper bounds of the joint $\Theta_i$;
- the *contact* penalty index:
$$\eta_C = \sqrt{d_{th}^2 + d_{ind}^2 + d_{mid}^2}, \qquad (11)$$
where $d_i$ is the distance in length between the point of contact on the fingertip $i$ and its center.

For each object of the set, we carried out 5 grasps, changing each time the starting hand pose.

Fig. 11 shows for each object the evolution of the penalty indexes while grasping adaptation is applied. The plot proves that the GMM regression actually manages to move the joints far from their bounds and the points of contact close to the center of the fingertips. In the case of the sponge, $\eta_C$ does not decrease considerably; this happens because the initial hand poses had already a good configuration. The variance related to $\eta_B$ strongly reduces over time for all the objects. This makes the method robust with respect to the initial hand pose. In the case of $\eta_C$, such effect is much lower, since the points of contact configuration is strongly dependent on the shape of the object and can be hard to control.

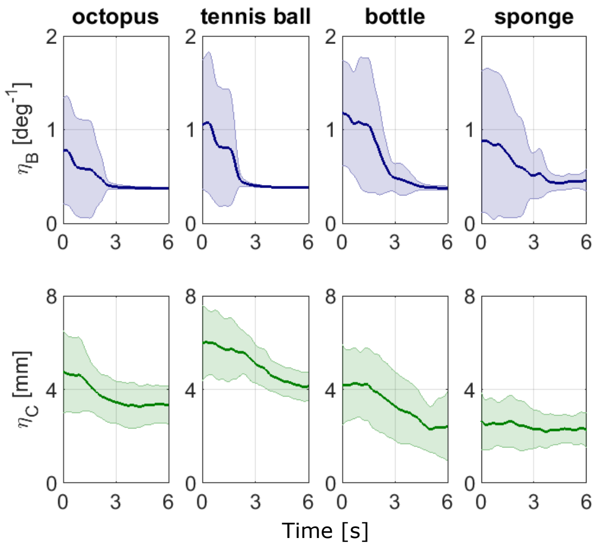


Fig. 11: Hand configuration penalties. The Figure shows, for each object, the mean and the confidence interval at 95% over the 5 grasps of the penalty indexes.

## IV. Conclusion

In this paper we dealt with active grasping adaption to unknown objects in order to improve stability. Our method is composed of three components: a low level force controllers framework, a high level controller that coordinates the fingers to achieve grasp stabilization and grip strength control, and a machine learning approach based on GMM regression aimed at further improving the grasp stability. The method is made simple and effective by taking advantage of the anthropomorphic structure of the hand. Furthermore, since forces are regulated by the high level controller, the amount of data needed for the GMM training is strongly reduced.

We tested our method on the iCub robot to demonstrate that our approach allows to reliably control the position of the object in the hand, while controlling the grip strength. Finally, we validated the re-grasp strategy provided by the GMM to demonstrate that it allows achieving grasp poses that are preferable for manipulation purposes and robust to perturbations.

The novelty of our work is that it performs grasp adaptation while allowing explicit control on the grip strength on the object using tactile feedback. Although not investigated in this paper, such feature can be useful in many applications. For example, it allows to adapt the grip-strengh to avoid slip while handling fragile objects or to squeeze the object to extract material properties for object recognition or subsequent in-hand manipulation.

## REFERENCES


[1] A. M. Okamura, N. Smaby, and M. R. Cutkosky, "An overview of dexterous manipulation," in *Robotics and Automation, 2000. Proceedings. ICRA'00. IEEE International Conference on*, vol. 1. IEEE, 2000, pp. 255–262.

[2] D. Prattichizzo and J. C. Trinkle, "Grasping," in *Springer handbook of robotics*. Springer, 2008, pp. 671–700.

[3] R. S. Dahiya, G. Metta, M. Valle, and G. Sandini, "Tactile sensingfrom humans to humanoids," *Robotics, IEEE Transactions on*, vol. 26, no. 1, pp. 1–20, 2010.

[4] H. Yussof, J. Wada, and M. Ohka, "Grasp synthesis based on tactile sensation in robot manipulation of arbitrary located object," in *2009 IEEE/ASME International Conference on Advanced Intelligent Mechatronics*. IEEE, 2009, pp. 560–565.

[5] K. Hsiao, S. Chitta, M. Ciocarlie, and E. G. Jones, "Contact-reactive grasping of objects with partial shape information," in *Intelligent Robots and Systems (IROS), 2010 IEEE/RSJ International Conference on*. IEEE, 2010, pp. 1228–1235.

[6] J. Felip and A. Morales, "Robust sensor-based grasp primitive for a three-finger robot hand," in *2009 IEEE/RSJ International Conference on Intelligent Robots and Systems*. IEEE, 2009, pp. 1811–1816.

[7] J. Schill, J. Laaksonen, M. Przybylski, V. Kyrki, T. Asfour, and R. Dillmann, "Learning continuous grasp stability for a humanoid robot hand based on tactile sensing," in *2012 4th IEEE RAS & EMBS International Conference on Biomedical Robotics and Biomechatronics (BioRob)*. IEEE, 2012, pp. 1901–1906.

[8] E. L. Sauser, B. D. Argall, G. Metta, and A. G. Billard, "Iterative learning of grasp adaptation through human corrections," *Robotics and Autonomous Systems*, vol. 60, no. 1, pp. 55–71, 2012.

[9] M. Li, Y. Bekiroglu, D. Kragic, and A. Billard, "Learning of grasp adaptation through experience and tactile sensing," in *2014 IEEE/RSJ International Conference on Intelligent Robots and Systems*. Ieee, 2014, pp. 3339–3346.

[10] R. Jakel, S. R. Schmidt-Rohr, Z. Xue, M. Losch, and R. Dillmann, "Learning of probabilistic grasping strategies using programming by demonstration," in *Robotics and Automation (ICRA), 2010 IEEE International Conference on*. IEEE, 2010, pp. 873–880.

[11] J. Tegin, S. Ekvall, D. Kragic, J. Wikander, and B. Iliev, "Demonstration-based learning and control for automatic grasping," *Intelligent Service Robotics*, vol. 2, no. 1, pp. 23–30, 2009.

[12] H. Dang and P. K. Allen, "Grasp adjustment on novel objects using tactile experience from similar local geometry," in *2013 IEEE/RSJ International Conference on Intelligent Robots and Systems*. IEEE, 2013, pp. 4007–4012.

[13] J. Jalani, N. Mahyuddin, G. Herrmann, and C. Melhuish, "Active robot hand compliance using operational space and integral sliding mode control," in *2013 IEEE/ASME International Conference on Advanced Intelligent Mechatronics*. IEEE, 2013, pp. 1749–1754.

[14] T. Feix, R. Pawlik, H.-B. Schmiedmayer, J. Romero, and D. Kragic, "A comprehensive grasp taxonomy," in *Robotics, Science and Systems: Workshop on Understanding the Human Hand for Advancing Robotic Manipulation*, 2009, pp. 2–3.

[15] G. Metta, G. Sandini, D. Vernon, L. Natale, and F. Nori, "The icub humanoid robot: an open platform for research in embodied cognition," in *Proceedings of the 8th workshop on performance metrics for intelligent systems*. ACM, 2008, pp. 50–56.

[16] V. Mathiowetz, N. Kashman, G. Volland, K. Weber, M. Dowe, S. Rogers *et al.*, "Grip and pinch strength: normative data for adults," *Arch Phys Med Rehabil*, vol. 66, no. 2, pp. 69–74, 1985.

[17] N. Jamali, M. Maggiali, F. Giovannini, G. Metta, and L. Natale, "A new design of a fingertip for the icub hand," in *IEEE/RSJ International Conference on Intelligent Robots and Systems*, 2015, pp. 2705–2710.